

DYNAMICAL FRICTION OF DOUBLE PERTURBERS IN A GASEOUS MEDIUM

HYOSUN KIM¹, WOONG-TAE KIM¹, AND F. J. SÁNCHEZ-SALCEDO²

Draft version April 12, 2008

ABSTRACT

In many astrophysical situations, as in the coalescence of supermassive black hole pairs at gas rich galactic nuclei, the dynamical friction experienced by an object is a combination of its own wake as well as the wakes of its companions. Using a semi-analytic approach, we investigate the composite wake due to, and the resulting drag forces on, double perturbers that are placed at the opposite sides of the orbital center and move on a circular orbit in a uniform gaseous medium. The circular orbit makes the wake of each perturber asymmetric, creating an overdense tail at the trailing side. The tail not only drags the perturber backward but it also exerts a positive torque on the companion. For equal-mass perturbers, the positive torque created by the companion wake is, on average, a fraction $\sim 40-50\%$ of the negative torque created by its own wake, but this fraction may be even larger for perturbers moving subsonically. This suggests that the orbital decay of a perturber in a double system, especially in the subsonic regime, can take considerably longer than in isolation. We provide the fitting formulae for the forces due to the companion wake and discuss our results in light of recent numerical simulations for mergers of binary black holes.

Subject headings: binaries : general — black hole physics — hydrodynamics — waves

1. INTRODUCTION

Understanding the nature of the dynamical friction (DF) force is of great importance to describe the evolution of gravitational systems. Although the concept of DF was introduced by Chandrasekhar (1943) studying collisionless backgrounds, it is also of astrophysical interest when considering gaseous media (e.g. Dokuchaev 1964; Ruderman & Spiegel 1971; Rephaeli & Salpeter 1980; Ostriker 1999; Sánchez-Salcedo & Brandenburg 1999, 2001). In a seminal paper, Ostriker (1999) derived the analytic formulae for drag forces on a perturber moving straight in a uniform gaseous medium, which have found a variety of astrophysical applications, from accretion disks (e.g. Narayan 2000; Karas & Šubr 2001; Chang 2001) to the intracluster medium (e.g., Kim et al. 2005; Kim 2007; Conroy & Ostriker 2008). Recently, Kim & Kim (2007, hereafter Paper I) extended the work of Ostriker (1999) to a more realistic case where the perturber moves on a circular orbit (see Barausse 2007 for the relativistic case).

Although the works mentioned above have improved our understanding on DF force on a single object, there are many astronomical situations involving double or multiple bodies in which one needs an analytical estimate of the net drag force. While the orbital evolution of a binary system due to the DF in a collisionless system has been studied in great detail (e.g., Heggie 1975), it is still lacking for the gaseous case. The latter is crucial to describe the formation and hardening of close binary systems (Bate et al. 2002), merging of double black holes at galactic centers (Escala et al. 2004, 2005; Dotti et al. 2006, 2007; Mayer et al. 2007), and orbital decays of kpc-sized giant clumps formed in primordial “clump cluster” galaxies (Immeli et al. 2004; Bournaud et al. 2007). In particular, angular momentum loss to gas provides a plausible mechanism to explain the rel-

atively rapid coalescence of supermassive black hole pairs in galaxy centers (e.g., Begelman et al. 1980; Gould & Rix 2000; Armitage & Natarajan 2002, 2005). Escala et al. (2004, 2005) found, through numerical simulations, that the black holes produce a composite wake of an inclined ellipsoidal shape that exerts a net torque on the black holes. This clearly indicates that the in-spiral of one black hole is affected also by the wake from its companion. In this *Letter*, we consider a system composed of two perturbers on coplanar circular orbits in order to assess quantitatively the effect of the companion wake. Using a semi-analytic approach, we study the structure of the combined density wake, evaluate the resulting drag force on each object, and apply our results to the cases considered in numerical simulations of DF-induced mergers of black holes.

2. FORMULATION

We consider two point-mass perturbers moving on coplanar circular orbits around the same orbital center in an inviscid gaseous medium.³ In order to isolate the effects of the companion, we assume a perfectly uniform background with density ρ_0 and ignore the complications from density gradients. To simplify the presentation further, we consider that both perturbers orbit with a fixed radius R_p and at a constant velocity V_p , and are located at the opposite sides of the orbital center, but the extension to general case is straightforward. To study the response of gas to the perturbers, we employ the same formalism as in Paper I for a time-dependent linear perturbation analysis. The reader is referred to Paper I for a more detailed description of the method.

Assuming that the perturbed density $\alpha = (\rho - \rho_0)/\rho_0$ is adiabatic and very small, we linearize the equations of hydrodynamics to obtain a three-dimensional wave equation

$$\nabla^2 \alpha - \frac{1}{c_s^2} \frac{\partial^2 \alpha}{\partial t^2} = -\frac{4\pi G}{c_s^2} \rho_{\text{ext}}(\mathbf{x}, t), \quad (1)$$

³ The perturbers may orbit under a common external gravitational potential and/or under their mutual gravity. They constitute a binary if the latter dominates.

¹ Department of Physics and Astronomy, FPRD, Seoul National University, Seoul 151-742, Korea; hkim@astro.snu.ac.kr, wkim@astro.snu.ac.kr

² Instituto de Astronomía, Universidad Nacional Autónoma de México, Ciudad Universitaria, 04510 Mexico City, Mexico; jsanchez@astroscu.unam.mx

where c_s is the adiabatic speed of sound in the unperturbed medium and ρ_{ext} denotes the mass density of the perturbers (e.g., Ostriker 1999).

We work in cylindrical coordinates (R, φ, z) with its origin lying at the orbital center and the z -axis perpendicular to the orbital plane. Assuming that the perturbers with mass M_p and fM_p each (with f denoting the mass ratio) are introduced at $(R_p, 0, 0)$ and $(R_p, \pi, 0)$ at $t = 0$, respectively, one can write

$$\rho_{\text{ext}}(\mathbf{x}, t) = M_p \mathcal{H}(t) \delta(R - R_p) \delta(z) \times \{ \delta[R_p(\varphi - \Omega t)] + f \delta[R_p(\varphi - \pi - \Omega t)] \}, \quad (2)$$

where $\mathcal{H}(t)$ is the Heaviside step function and $\Omega \equiv V_p/R_p$ is the angular speed of the perturbers. Since equation (1) is linear, α is given by a simple superposition of the wakes of both perturbers. By solving equation (1) based on the retarded Green's function technique and simplifying the resulting integral analytically, one can show that the perturbed density is reduced to

$$\alpha(\mathbf{x}, t) = \frac{GM_p}{c_s^2 R_p} \mathcal{D}(R, \varphi, z, t), \quad (3)$$

where $\mathcal{D} = \mathcal{D}_1 + f \mathcal{D}_2$ with \mathcal{D}_1 and \mathcal{D}_2 denoting the dimensionless wake, given by equation (8) in Paper I, of the perturber with mass M_p and fM_p , respectively. Note that $\mathcal{D}_2(R, \varphi, z, t) = \mathcal{D}_1(R, \varphi - \pi, z, t)$ for the perturbers in consideration.

The gravitational drag force exerted on the perturber of mass M_p located at the position \mathbf{x}_p can be obtained by directly evaluating the integral

$$\mathbf{F}_{\text{DF}} = GM_p \rho_0 \int d^3 \mathbf{x} \frac{\alpha(\mathbf{x}, t) (\mathbf{x} - \mathbf{x}_p)}{|\mathbf{x} - \mathbf{x}_p|^3} = \mathbf{F}_{\text{DF},1} + \mathbf{F}_{\text{DF},2}, \quad (4)$$

where $\mathbf{F}_{\text{DF},1} = -\mathcal{F}(\mathcal{I}_{1,R} \hat{\mathbf{R}} + \mathcal{I}_{1,\varphi} \hat{\boldsymbol{\varphi}})$ and $\mathbf{F}_{\text{DF},2} = -\mathcal{F}f(\mathcal{I}_{2,R} \hat{\mathbf{R}} + \mathcal{I}_{2,\varphi} \hat{\boldsymbol{\varphi}})$, with $\mathcal{F} \equiv 4\pi\rho_0 (GM_p/V_p)^2$. Here, $\hat{\mathbf{R}}$ represents the unitary direction vector along R , and $\mathcal{I}_{1,R}$ and $\mathcal{I}_{1,\varphi}$ are the dimensionless drag forces on a perturber by its own wake in the radial and azimuthal directions, respectively, while $\mathcal{I}_{2,R}$ and $\mathcal{I}_{2,\varphi}$ refer to those from the wake of its companion with mass fM_p . The former was evaluated and widely discussed in Paper I. We here focus on $\mathcal{I}_{2,R}$ and $\mathcal{I}_{2,\varphi}$ defined by equations (12) of Paper I except \mathcal{D}_2 replacing \mathcal{D} for the perturbed density.

As in Paper I, we calculate $\mathcal{D}(\mathbf{x}, t)$ and \mathbf{F}_{DF} on a three-dimensional Cartesian mesh centered at the center of the orbit. We checked that the grid spacing of $\sim R_p/640$ and the box size of $\sim (20-100) R_p$ are sufficient to give converged results.

3. RESULTS

3.1. Density Wake

In this section, we limit our presentation to the cases with equal-mass perturbers; the cases with $f \neq 1$ will be briefly discussed in §4. As the perturbers introduced at $t = 0$ move along a circular orbit, they continuously launch sound waves that propagate and affect the surrounding medium that would otherwise be uniform and static. Any location inside the causal region is able to receive sonic perturbations from both perturbers, possibly multiple times, creating a density wake that differs significantly depending on the Mach number $\mathcal{M} \equiv V_p/c_s$ of the perturbers. Figure 1 displays the distributions of the dimensionless wake \mathcal{D} on the orbital plane ($z = 0$), when a steady state is reached ($t \gg R_p/c_s$) for $\mathcal{M} = 0.6, 1.2, 2.0$, and 3.2 . In each frame, the perturbers located at $(x, y) = (\pm R_p, 0)$ are rotating counterclockwise.

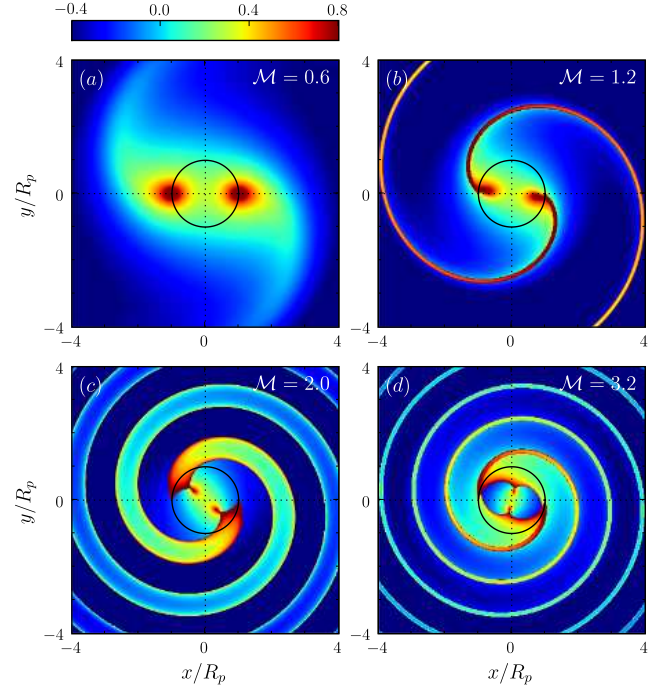


FIG. 1.— Distributions of the dimensionless perturbed density \mathcal{D} in a steady state for (a) $\mathcal{M} = 0.6$, (b) 1.2 , (c) 2.0 , and (d) 3.2 on the orbital plane ($z = 0$). The perturbers of equal mass located at $(x, y) = (\pm R_p, 0)$ are moving in the counterclockwise direction along a circular orbit marked by the black circle in each frame. Colorbar labels $\log \mathcal{D}$.

For subsonic perturbers ($\mathcal{M} < 1$), the perturbed density is smooth without involving a shock. The bending of the wakes caused by the circular motions leads to slight over-densities at the trailing sides (see Fig. 1a), producing nonvanishing drag forces. In the steady state, which is achieved at $t \rightarrow \infty$, a parcel of gas at any position receives one sonic perturbation from each perturber. For supersonic cases ($\mathcal{M} > 1$), on the other hand, the wake of each perturber initially consists of a sonic sphere and a Mach cone, the interiors of which are influenced by sonic disturbances once and twice, respectively. Because of the circular motion, a perturber (and the head of its Mach cone) is able to overtake its own sonic sphere and subsequently the other sonic sphere from the companion, both of which are expanding radially outward. This in turn provides additional perturbations to the wakes and thus forms long high-density tails that loosely wrap the perturbers in a trailing spiral fashion, as Figure 1 shows. The tails in fact trace the regions bounded by shock discontinuities where the gas has received sonic signals four times (three from one perturber and one from the other) and do not overlap with each other, provided the Mach number is less than 2.972 (see below). Note that the densest parts of a tail are located at the immediate trailing side of a perturber, which indicates that the companion wake generally tends to reduce the net DF force, as we shall show in §3.2.

The wake tails thicken as the Mach number increases from unity. Paper I showed that a tail from a single perturber becomes fat enough to make the inner edge contact with the outer edge at $\mathcal{M}_1 = 4.603$. The self-overlapping of a tail develops a new thin tail that becomes thicker with increasing \mathcal{M} and again overlaps itself at $\mathcal{M}_2 = 7.790$, and so on. In double-perturber cases, however, one tail is able to mutually overlap with the other even before it undergoes self-overlapping. The critical Mach numbers \mathcal{M}_n for the mutual overlapping of tails are determined by equation (B3) in Paper I for half-

integer n . A few critical Mach numbers are $\mathcal{M}_{1/2} = 2.972$, $\mathcal{M}_{3/2} = 6.202$, and $\mathcal{M}_{5/2} = 9.371$. The high-density narrow tails shown in Figure 1d for $\mathcal{M} = 3.2$ are constructed by combining six sonic disturbances emitted by the perturbers.

3.2. Gravitational Drag Force

Once the perturbed density $\mathcal{D}(\mathbf{x}, t)$ is constructed, it is straightforward to calculate the DF forces exerted on each perturber. While the volume of space influenced by the perturbers steadily increases with time, the resulting drag forces quickly converge to their steady-state values typically within one orbital period. Figure 2 plots the various drag forces in a steady state on a perturber as functions of the Mach number. In order to avoid a divergence of the force integral, only the region with the distance $r > r_{\min} = R_p/10$ from the perturber is taken into account in the force computation. Note that only $\mathcal{I}_{1,\varphi}$ depends on the Coulomb logarithm $\ln(r_{\min}/R_p)$ for supersonic perturbers; the other three forces ($\mathcal{I}_{1,R}$, $\mathcal{I}_{2,R}$, and $\mathcal{I}_{2,\varphi}$) are independent of the adopted value for r_{\min} . The local bumps in $\mathcal{I}_{2,R}$ and $\mathcal{I}_{2,\varphi}$ are caused by the overlapping of the tails occurring at the critical Mach numbers, as discussed in §3.1.

Figure 2 shows that $\mathcal{I}_{2,\varphi}$ has opposite sign to $\mathcal{I}_{1,\varphi}$ for all \mathcal{M} . This implies that, regardless of the Mach number, one perturber in a double-perturber system gains angular momentum from the gravitational torque exerted by the companion wake, while its own wake always takes away angular momentum from it. For equal-mass perturbers, the net drag force in the azimuthal direction is thus smaller than the isolated counterpart. The contribution of the companion wake to the DF force in the azimuthal direction is delineated in the inset of Figure 2. In the supersonic range, the ratio $-\mathcal{I}_{2,\varphi}/\mathcal{I}_{1,\varphi}$ is on average $\sim 40\%$, and drops to $\sim 12\%$ at $\mathcal{M} \sim 1.2-1.4$ where the net azimuthal drag force is maximized. Since $\mathcal{I}_{1,\varphi}$ increases with decreasing $\ln(r_{\min}/R_p)$ for $\mathcal{M} > 1$, the effect of the companion wake on the orbital decay of supersonic double perturbers would diminish as the perturber size nominally represented by r_{\min} decreases relative to the orbital radius. Interestingly, in the subsonic case, the ratio $-\mathcal{I}_{2,\varphi}/\mathcal{I}_{1,\varphi}$, which does not depend on r_{\min} , is $\sim 50\%$ at $\mathcal{M} \sim 0.7$ and steeply approaches unity as $\mathcal{M} \rightarrow 0$, suggesting that the effect of the companion wake is larger as the speed of perturbers decreases.

On the other hand, $\mathcal{I}_{1,R}$ and $\mathcal{I}_{2,R}$ are of comparable amplitude over a wide range of \mathcal{M} , and thus give rise to a net radial drag on double perturbers that is about twice larger than in the corresponding single-perturber cases⁴. They affect the orbital eccentricity rather than removing angular momentum much (e.g., Paper I), which may have a gravitational wave signature detectable with *Laser Interferometer Space Antenna (LISA)* (Armitage & Natarajan 2005).

For practical purposes, we fit our results for $\mathcal{I}_{2,R}$ and $\mathcal{I}_{2,\varphi}$ using

$$\frac{\mathcal{I}_{2,R}}{\mathcal{M}^2} = \begin{cases} 0.5 - 0.43 \left(1 - \cosh^{-0.36}(2.2\mathcal{M})\right) & \text{if } \mathcal{M} < 2.97, \\ 0.76 - 0.08 \left(\mathcal{M} + (\mathcal{M} - 2.76)^{-1}\right) & \text{if } 2.97 \leq \mathcal{M} < 6.2, \\ 0.56 - 0.027 \left(\mathcal{M} + (\mathcal{M} - 6)^{-1}\right) & \text{if } \mathcal{M} \geq 6.2, \end{cases} \quad (5)$$

⁴ When $\mathcal{M} = 0$, the steady-state solution of equation (1) is simply $\alpha = (GM_p/c_s^2)(|r - R_p|^{-1} + f|r + R_p|^{-1})$, for which equation (4) yields $\mathcal{I}_{2,R}/\mathcal{M}^2 = 0.5$ and $\mathcal{I}_{2,\varphi}/\mathcal{M}^2 = 0$.

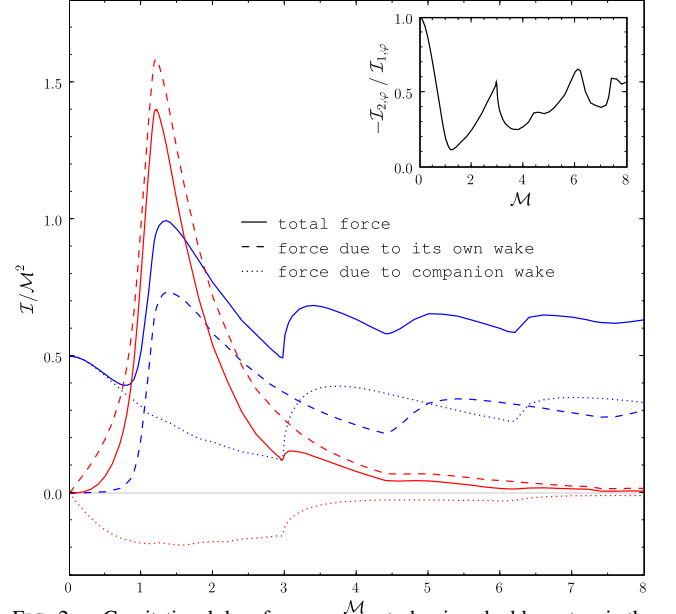


FIG. 2.— Gravitational drag forces on a perturber in a double system in the radial (blue) and azimuthal (red) directions as functions of the Mach number \mathcal{M} . The dashed curves adopted from Paper I with $r_{\min}/R_p = 0.1$ represent the forces (\mathcal{I}_1) originated from the wake of the perturber itself, while those (\mathcal{I}_2) from the companion wake are plotted as dotted lines. The solid lines give the net DF forces ($\mathcal{I}_1 + \mathcal{I}_2$) for equal-mass perturbers. The inset plots the ratio $-\mathcal{I}_{2,\varphi}/\mathcal{I}_{1,\varphi}$ which is positive and less than unity for all \mathcal{M} .

$$\frac{\mathcal{I}_{2,\varphi}}{\mathcal{M}^2} = \begin{cases} -0.022(10 - \mathcal{M}) \tanh(3\mathcal{M}/2) & \text{if } \mathcal{M} < 2.97, \\ -0.13 + 0.07 \tan^{-1}(5\mathcal{M} - 15) & \text{if } \mathcal{M} \geq 2.97, \end{cases} \quad (6)$$

which are accurate within 6% of the numerical results for all \mathcal{M} . The algebraic fits to $\mathcal{I}_{1,R}$ and $\mathcal{I}_{1,\varphi}$ are given by equations (13) and (14) of Paper I. It can be shown that $\mathcal{I}_{1,\varphi} \approx -\mathcal{I}_{2,\varphi} \rightarrow \mathcal{M}^3/3$ in the limit of small \mathcal{M} .

4. DISCUSSION

For a system composed of two perturbers moving on coplanar circular orbits at the opposite sides of the system center, we have found that a perturber is dragged backward by its own induced wake, while it is simultaneously pulled forward by the wake of its companion. For equal-mass perturbers, the ratio of the positive torque from the companion wake to the negative torque from its own wake varies between 0.1 to 1.0, and has a mean value at about 0.4. This indicates that, since the wake tails are a large-scale perturbation, the effect of a companion wake on the orbital decay of a double system is by no means negligible except perhaps at $\mathcal{M} \sim 1.2-1.4$. When the perturbers do not have the same orbital radius, the positive torque generated by the companion wake is expected to be enhanced (thus making the net azimuthal drag reduced) if the companion has a larger orbital radius. In order to quantify this effect, we have computed the drag force, for instance, on a body with $\mathcal{M} = 1$ at R_p when the companion is at $2R_p$ and $\mathcal{M} = 2$ (in order to have the same Ω), and found that the positive torque increases by a factor of ~ 1.4 . If the perturbers have different orbital frequencies so that one perturber completes several orbits in the orbital period of the companion, the orbit-averaged torque exerted by the wake of the companion is likely to be reduced. In the limit of very different frequencies, the orbit-averaged torque by the companion wake becomes negligible.

The results of this *Letter* can be immediately applied to the numerical models considered in Escala et al. (2004) for DF-induced mergers of supermassive black holes in a gaseous

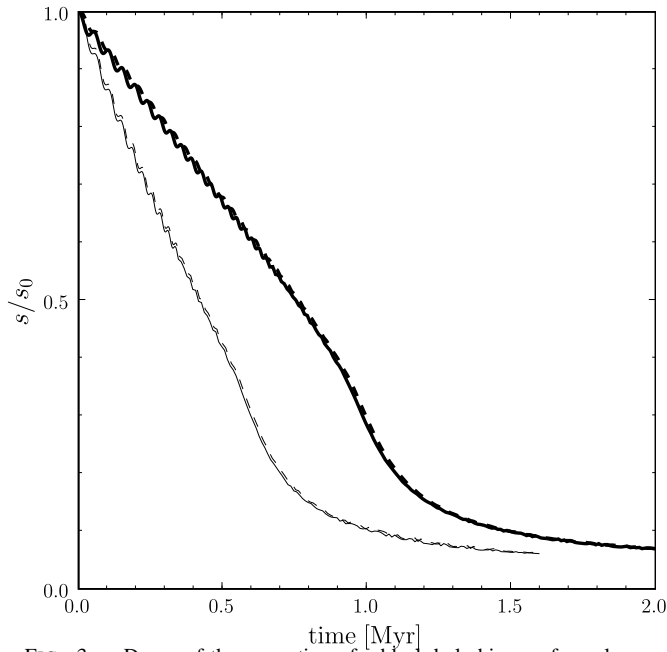


FIG. 3.— Decay of the separation of a black hole binary of equal mass caused by dynamical friction due to a background gas. The thick and thin curves correspond to the cases when the wakes of both binary components are considered and when the companion wake is ignored, respectively. In both cases, the solid lines plot the results based on both radial and azimuthal forces, while those with only azimuthal forces are given as dashed lines.

medium. In their model, two black holes of equal mass are initially separated from each other widely and orbit at near-transonic speed under an external gravitational potential and begin to undergo gaseous drag. Our results shown in Figure 2 suggest that the companion wake presumably plays a minor role in this early phase of the orbital decay. Escala et al. (2004) reported that at some point when the binary separation is reduced to ~ 7 pc, the binary produces a wake in the surrounding medium that is well approximated by an ellipsoid with an axis ratio of 2:1. The major axis of the ellipsoid lags behind the binary axis by $\sim 22.5^\circ$. Since the wake configuration of this sort can be obtained by blurring the perturbed density shown in Figure 1a, we infer that the black holes have $\mathcal{M} \sim 0.6$ at this time. The binary keeps hardening by an ellipsoidal torque, and the effect of the companion wake is now non-negligible at all.

Figure 10 of Escala et al. (2004) shows that it takes the binary about 1.5 Myr to decay from 7 to 0.7 pc. To check

whether this is consistent with our predictions, we consider a binary black hole with mass $M_p = 5 \times 10^8 M_\odot$ each, embedded in a uniform medium with number density $n_0 = 1.5 \times 10^5 \text{ cm}^{-3}$ and sound speed $c_s = 650 \text{ km s}^{-1}$, a condition similar to those in Escala et al. (2004). Initially, the binary has $\mathcal{M} = 0.6$ and a separation of $s_0 = 7$ pc. We follow the orbital decay of the binary subject to the DF forces found in §3.2. Figure 3 plots the resulting temporal changes of the separation s . The thick curves correspond to the cases when the wakes of both binary components are considered, which show that the binary decays to $s = 0.7$ pc in ~ 1.5 Myr, consistent with the results of Escala et al. (2004). When the effects of the companion wake are neglected, the decay time becomes shorter by about a factor of 1.5, as indicated by the thin lines. Note that the close agreement between the two cases with and without the radial force demonstrates that it does not affect the decay much.

The fact that the companion wake always acts against the orbital decay of a double system suggests an interesting possibility that a less massive perturber in an unequal-mass system may be able to experience a forward net force and move radially outward by acquiring (instead of losing) angular momentum from the wake of a more massive body, resembling a dynamical barrier, while the latter is little influenced by the former. This *dynamical boost* happens if the mass ratio f of two components exceeds $|\mathcal{I}_{1,\varphi}/\mathcal{I}_{2,\varphi}|$. The evolution of unequal-mass perturbers is more complex since the assumption of identical orbits for both perturbers will fail soon. In practice, one expects that the orbit of the light perturber will be quenched to the massive perturber; the former is trapped on a radius where the drag of its own wake is slightly larger than the forward force of the companion wake, until the orbit of the massive perturber decays and the wakes decouple. We will discuss this case somewhere else.

We are grateful to an anonymous referee for a thoughtful report. This work was supported by KICOS through the grant K20702020016-07E0200-01610 provided by MOST, and partly for H.K. by the BK21 project of the Korean Government. The computations were performed on the Linux cluster at the KASI built with funding from KASI and the ARCSEC. F.J.S.S. acknowledges financial support from projects PAPIIT IN114107 and CONACyT 60526.

REFERENCES

- Armitage, P. J., & Natarajan, P. 2002, *ApJ*, 567, L9
 Armitage, P. J., & Natarajan, P. 2005, *ApJ*, 634, 921
 Barausse, E. 2007, *MNRAS*, 382, 826
 Bate, M. R., Bonnell, I. A., & Bromm, V. 2002, *MNRAS*, 336, 705
 Begelman, M. C., Blandford, R. D., & Rees, M. J. 1980, *Nature*, 287, 307
 Bounaud, F., Elmegreen, B. G., & Elmegreen, D. M. 2007, *ApJ*, 670, 237
 Chandrasekhar, S. 1943, *ApJ*, 97, 255
 Chang, H.-Y. 2001, *ApJ*, 551, L159
 Conroy, C., & Ostriker, J. P. 2008, *ApJ*, in press; astro-ph/0712.0824
 Dokuchaev, V. P. 1964, *Soviet Astron.*, 8, 23
 Dotti, M., Colpi, M., & Haardt, F. 2006, *MNRAS*, 367, 103
 Dotti, M., Colpi, M., Haardt, F., & Mayer, L. 2007, *MNRAS*, 369, 956
 Escala, A., Larson, R. B., Coppi, P. S., & Mardones, D. 2004, *ApJ*, 607, 765
 Escala, A., Larson, R. B., Coppi, P. S., & Mardones, D. 2005, *ApJ*, 630, 152
 Gould, A., & Rix, H.-W. 2000, *ApJ*, 532, L29
 Heggie, D. C. 1975, *MNRAS*, 173, 729
 Immeli, A., Samland, M., Gerhard, O., & Westera, P. 2004, *A&A*, 413, 547
 Karas, V., Šubr, L. 2001, *A&A*, 376, 686
 Kim, W.-T. 2007, *ApJ*, 667, L5
 Kim, W.-T., El-Zant, A. A., & Kamionkowski, M. 2005, *ApJ*, 632, 157
 Kim, H., & Kim, W.-T. 2007, *ApJ*, 665, 432 (Paper I)
 Mayer, L., Kazantzidis, S., Madau, P., Colpi, M., Quinn, T., & Wadsley, J. 2007, *Science*, 316, 1874
 Narayan, R. 2000, *ApJ*, 536, 663
 Ostriker, E. C. 1999, *ApJ*, 513, 252
 Rephaeli, Y., & Salpeter, E. E. 1980, *ApJ*, 240, 20
 Ruderman, M. A., & Spiegel, E. A. 1971, *ApJ*, 165, 1
 Sánchez-Salcedo, F. J., & Brandenburg, A. 1999, *ApJ*, 522, L35
 Sánchez-Salcedo, F. J., & Brandenburg, A. 2001, *MNRAS*, 322, 67